Transactions, **SMiRT-26**
Berlin/Potsdam, Germany, July 10-15, 2022
Division V

Geometric influences on the behaviour of beams under impact loading

Lena Leicht[1], Petr Máca[2], Birgit Beckmann[3], Manfred Curbach[4]

[1] Dipl.-Ing., TU Dresden, Dresden (lena.leicht@tu-dresden.de)
[2] PhD, TU Dresden, Dresden
[3] Dr.-Ing., TU Dresden, Dresden
[4] Univ.-Prof. Dr.-Ing. Dr.-Ing. E.h., TU Dresden, Dresden

ABSTRACT

The aim of this contribution is to highlight the difference in the behaviour of beams with and without stirrup reinforcement under hard impact loading. A comparison is drawn considering the cracking and damage process, the deformations and accelerations, the support forces, and the strains measured on the reinforcement bars during the impact. It was found that the cracks of the stirrup-reinforced beams were finer distributed than in the case without stirrup reinforcement. Especially the crack between punching cone and residual section had a smaller crack-opening width, meaning the specimen remained one solid body. Above that, the burst mass that spalled off on the top side of the specimen was generally smaller for stirrup-reinforced beams. The support forces of the stirrup-reinforced beams were higher. The strains over time also varied between beams with and without stirrup reinforcement as the latter had a longer strain plateau and residual vibrations were recorded after the impact.

INTRODUCTION

Nuclear power plants (NPP) belong to the so-called critical infrastructure. For that reason, higher standard of safety needs to be ensured. To guarantee the safety of concrete structures, impact tests on specimens are necessary. Many impact experiments on beam specimens were carried out with heavy impactors at low impact velocities or with servo-controlled rapid loading machines and a deformation control. Somraj et al. (2013) used a servo-hydraulic rapid loading machine in their experiments. The maximum impact force the machine can apply is 980 kN and the maximum loading rate is 4 m/s. A steel plate with a height of 40 mm was placed between the impactor and the specimen. They tested beams with spans of 1000 mm and 1400 mm at constant deflection rates. They varied the shear reinforcement ratio and found that a higher reinforcement ratio led to a more ductile failure mode. Saatci and Vecchio (2009) used heavy impactors of 211 kg and 600 kg at small loading velocities of about 8 m/s to impact their specimens with 3000 mm span length. Most of their specimens showed a shear failure mode. Soleimani and Sayyar Roudsari (2019) also used a heavy impactor of 591 kg at a velocity of only 7 m/s. They also found shear failure as the main failure mode in their experiments. In the experiments of Zhan et al. (2015) soft impact conditions were created with the help of rubber pads leading to a wide bending crack in the centre of the beams. The tested beams had spans of 1200 mm with an impactor mass of only 33.6 kg.
By contrast with the aforementioned experiments, the following experiments were carried out under hard impact conditions at a short loading duration. This is achieved by small impactor masses which are accelerated by compressed air to achieve velocities of up to 30 m/s. Besides other measurements taken along the beams, multiple strain measurements were taken along the reinforcement bars. This gives additional insight into the beam specimens and distinguishes this research from the aforementioned. A comparison of the behaviour of specimens reinforced with different degrees of reinforcement was found to

be interesting in the cited literature. Thus, in the following, the behaviour of beams with and without stirrup reinforcement under high-velocity impact is compared.

MATERIALS AND METHODS

Beams with dimensions of 1500 mm length, 150 mm width and 300 mm height were cast of concrete in class C35/45. The cement used was of class CEM III. The longitudinal reinforcement bars had a diameter of 10 mm and the ductility class was B500 B. The beams were longitudinally reinforced with three reinforcement bars in the bottom layer and two reinforcement bars in the top layer. Some of the beams were additionally stirrup-reinforced. The stirrup diameter was 8 mm and the spacing was 100 mm or 200 mm. Drawings of the different specimens with strain gauge locations can be seen in Fig. 1.

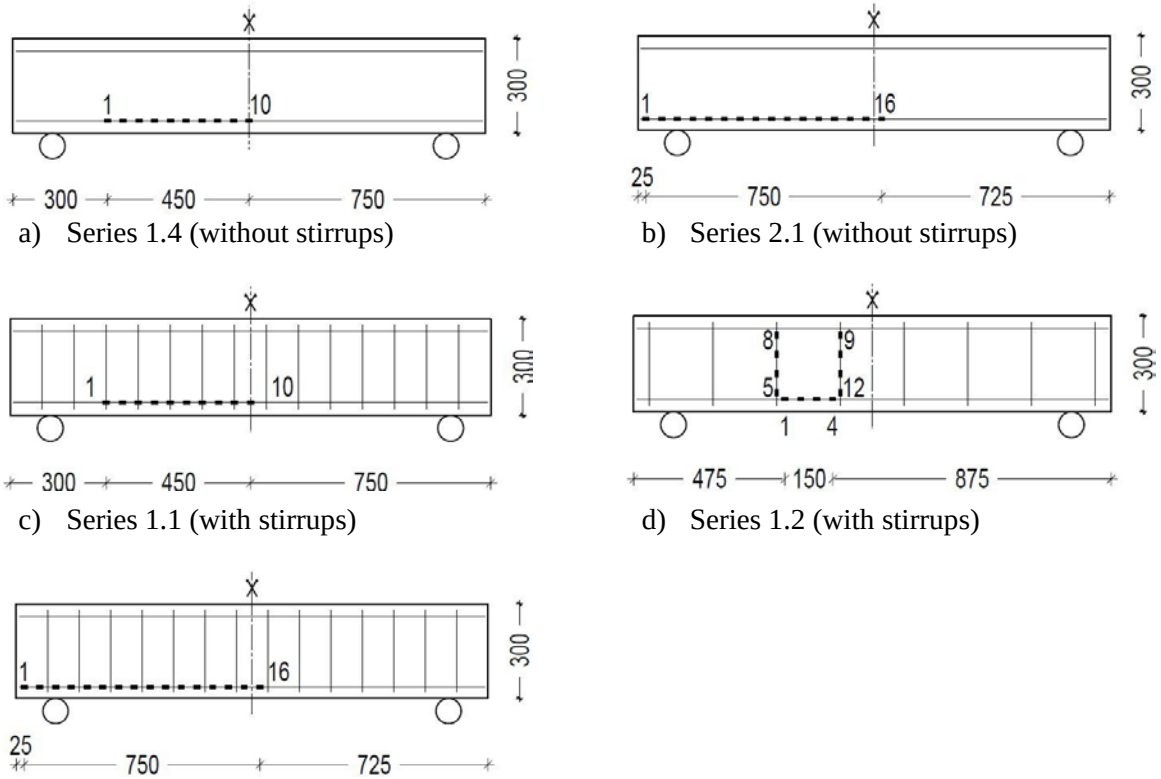

Figure 1. Geometry, reinforcement, and strain measurement positions for beams. (Leicht et al. (2021))

The experiments were carried out in the drop tower of the Otto-Mohr-Laboratory at TU Dresden. The setup of the drop tower is described in detail in Just et al. (2015) and Hering et al. (2017). Compressed air accelerated the impactor with a length of 250 mm to velocities between 18 m/s and 28.2 m/s. Before hitting the specimen, the impactor was guided in an 11 m-long steel tube.

The specimens were instrumented with assorted measurement equipment (see Fig. 2). Before casting the specimens, strain gauges were applied to different positions along the reinforcement bars. The positions of the strain gauges with 1 mm gauge length and 120 Ω resistance can be seen in Figure 1 (black rectangles). The strain gauges on the longitudinal reinforcement bars were all applied to the rebar in the centre of the specimen. They were furthermore applied on the side of the reinforcement bars to minimize bending influences on the strain gauge readings. Apart from the strain gauges on the rebars, four accelerometers (ACC1 to ACC4) measured the acceleration at different positions along the specimens.

Three of them were mounted at the top side of the specimen and the fourth measured the acceleration at the bottom in the middle of the specimen. The measured values of ACC4 were inverted to be directly comparable to the other three measurements. Additionally, two lasers (L1 and L2) measured the deflection in the middle and in the quarter-point of the span length. The Laser Doppler Vibrometer (LDV) measured the deflection of the specimen on the top side. The beams were simply supported and the support force was measured by two combined semiconductor and piezoelectric load cells.

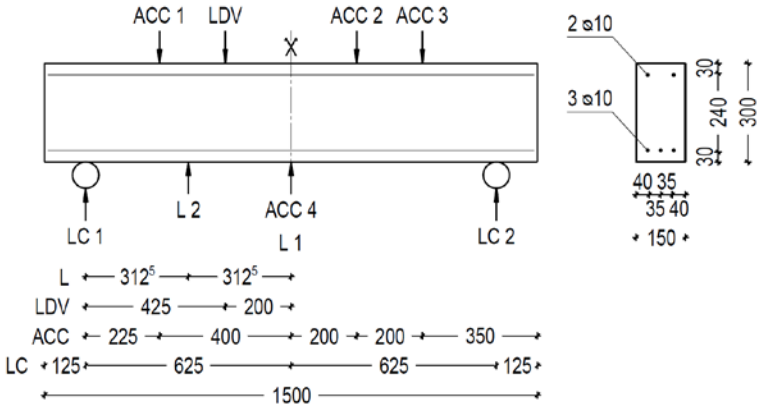

Figure 2. Instrumentation and reinforcement of the beams. Left: longitudinal section. Right: cross section. All lengths in mm. (Leicht et al. (2021))

RESULTS

Cracking and damage process

The impact of the steel impactor induced a compressive stress wave that traveled through the specimen. A punching cone, pointing to a shear failure, was the main failure mode in all conducted experiments. The typical inclined shear cracks were formed in all experiments. The first crack that occurred was, however, the bending crack in the centre of the beams. It had a very small crack width which is why it was in some cases hardly visible after the experiments. This crack started to form at about 0.2 ms to 0.3 ms after the impact of the steel projectile. Afterwards, 0.2 ms to 0.6 ms after the impact, the shear cracks started to appear. The main difference between the stirrup-reinforced beams and the beams without stirrup reinforcement lied in the crack distribution. The additional reinforcement led to a finer crack pattern as the stirrup reinforcement kept the specimens whole (see Fig. 3). That means that the stirrup reinforcement prevented the untying, and thus individual movement, of the punching cone from the rest of the specimen. At high velocities and without stirrup reinforcement, the punching cone was separated from the rest of the section, which can especially be seen in Fig. 3 b (Leicht et al (2020), Leicht et al. (2021)).

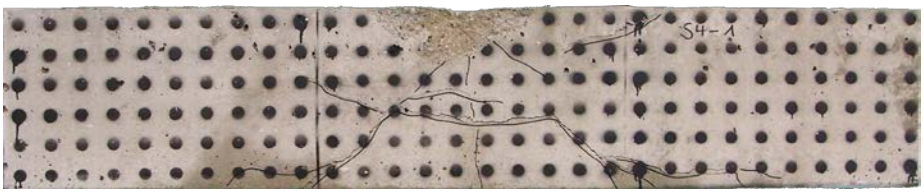

a) S1.4 (without stirrups) tested at 18.2 m/s.

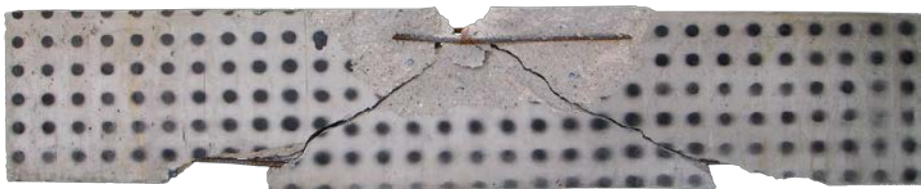

b) S2.1 (without stirrups) tested at 26.2 m/s.

c) S1.1 (with stirrups) tested at 19.0 m/s. Cracks are highlighted.

d) S1.2 (with stirrups) tested at 19.3 m/s. Cracks are highlighted.

e) S2.2 (with stirrups) tested at 28.2 m/s.

Figure 3. Crack pattern of different beams after the experiments. (Leicht et al. (2021))

When the compressive impact wave traveled through the specimen, it reached the bottom side of the specimen and is reflected as a tensile wave. The same is true for the transversely travelling waves. These were also reflected at the side of the beam and reflected as tensile waves. The sum of these tensile stress waves induced a bursting failure at the top of the specimens. The amount of burst mass depended on the geometry of the beam. It is generally smaller for the stirrup-reinforced beams because the internal part of the specimen, which is enclosed by the stirrup reinforcement, remained intact. In cases without stirrup reinforcement, more of the width of the beam is spalled off by tensile stresses. Additionally, some specimens without stirrup reinforcement also exhibited a scabbing failure at the bottom side (see Fig. 3 b) increasing the total spalling and scabbing mass (Leicht et al. (2021)).

Deformation and acceleration

As aforementioned, the deflection of the beams was measured directly by two lasers on the bottom side and a LDV on the top side of the specimen. For the beams with stirrup reinforcement, the deformation on top (LDV) and bottom side (laser) were similar. However, it was very different for beams without stirrup reinforcement. In this case, the amplitude of the deformation on the bottom side was a lot higher than the one of the deformation on the top side. This indicates that the punching cone was separated from the rest of the cross section and moved independently from the rest of the section. In the case of the stirrup-reinforced beams, by contrast, the punching cone was not untied from the rest of the section. With stirrup reinforcement, the specimens also bent back after the initial impact, leading to high positive deflections after the first negative peak. The specimens without stirrup reinforcement, by contrast, experienced residual deformations after the impact. Especially the punching cone remained only held by the longitudinal reinforcement. Exemplary plots are shown in Figure 4.

The maximum deformation on the top side always occurred earlier than the maximum deformation on the rear side. About 1.7 ms to 4.2 ms after the impact, the deformation on the top side reached its maximum of 2.8 mm to 7.5 mm. This maximum deformation increased with increasing impactor velocity but it was independent of the beam's reinforcement. The maximum deformations on the bottom side of the beams were smaller for the stirrup-reinforced beams. They were measured later after the impact and the time delay between the moment of impact and the moment of maximum deflection increased with increasing impactor velocity (Leicht et al. (2021)).

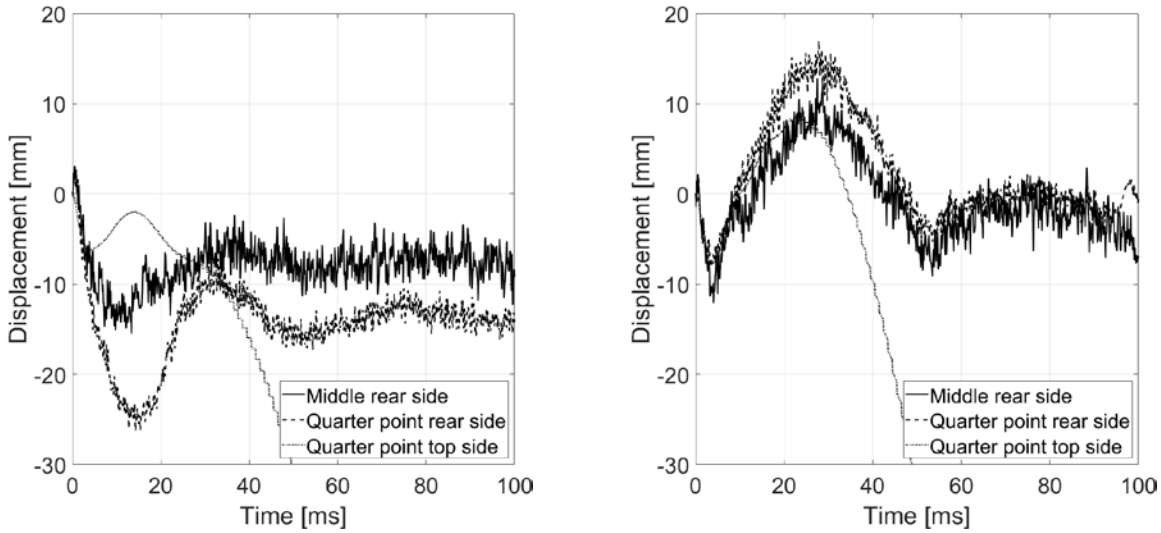

a) S2.1 (without stirrups) tested at 26.2 m/s b) S2.2 (with stirrups) tested at 28.2 m/s

Figure 4. Comparison of deflection of the beams with and without stirrup reinforcement.

To verify the observation of the laser and LDV measurements, the acceleration measurements were integrated twice after smoothing the curves. Of course, the results obtained by integrating measured values twice need to be handled with care and must be compared to other measurements. Indeed, the results were very similar to the ones obtained by the LDV and the lasers. For the beams without stirrup reinforcement, the deformation of the punching cone on the bottom side (ACC 4) exceeded the deformation on the top side (ACC 2). With additional stirrup reinforcement, the deformations measured on the top and the bottom side were very similar. The upward movement of the stirrup-reinforced beams subsequent to the impact was also indicated by the acceleration measurements of both ACC 2 and ACC 4. Above that, the time delays were also well visible and comparable to the ones seen in the direct measurement of the deformation by the LDV and the lasers (see Fig. 5 b) (Leicht et al. (2021)).

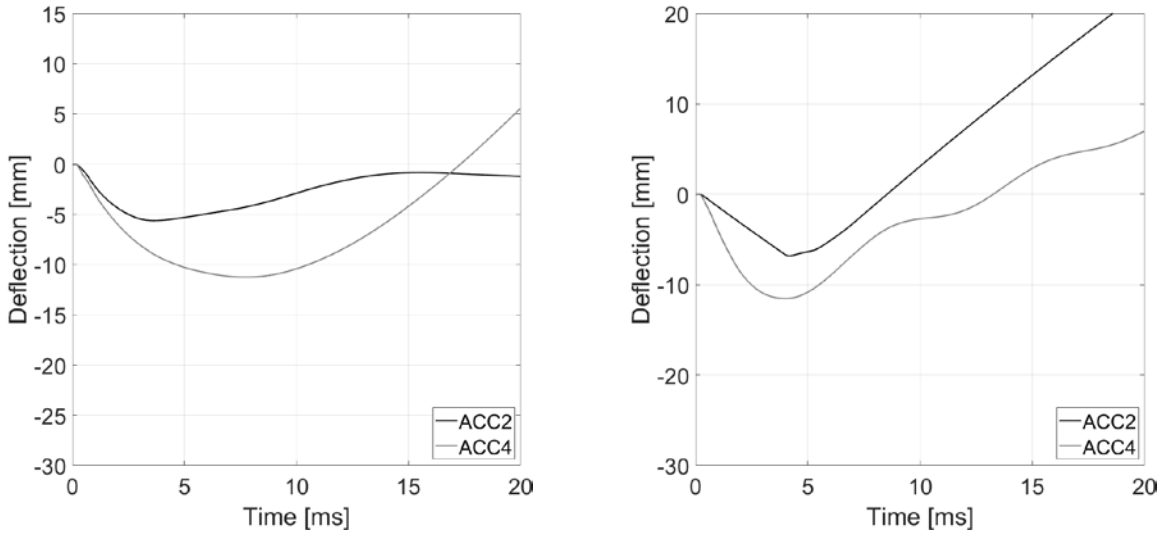

a) S2.1 (without stirrups) tested at 26.2 m/s b) S2.2 (with stirrups) tested at 28.2 m/s

Figure 5. Comparison of deflections derived from acceleration measurements of the beams with and without stirrup reinforcement.

The highest accelerations were measured on the punching cone on the bottom side by ACC 4. Oftentimes, the measured accelerations exceeded the sensor limit of 50,000 m/s^2 given by the producer. Above this limit, the measured accelerations are not reliable. Therefore, the measurements were cut off where the accelerations were above this limit. Thus, the maximum acceleration values of ACC 4 cannot be compared between the experiments. The maximum accelerations were always measured shortly after the impact. About 1.5 ms after the impact, the oscillations of the accelerations were already subsiding in all experiments (see Fig. 6). It is interesting to see that the accelerations of ACC 2 and ACC 4 started to occur simulateously while it took some time until the other two ACC stared measureing accelerations. This can be explained by the fact that ACC 2 and ACC 4 were closer to the impacted point than the other two accelerometers. It thus takes some time for the strain wave to reach the other two measurement positions of ACC 1 and ACC 3 (Leicht et al. (2021)).

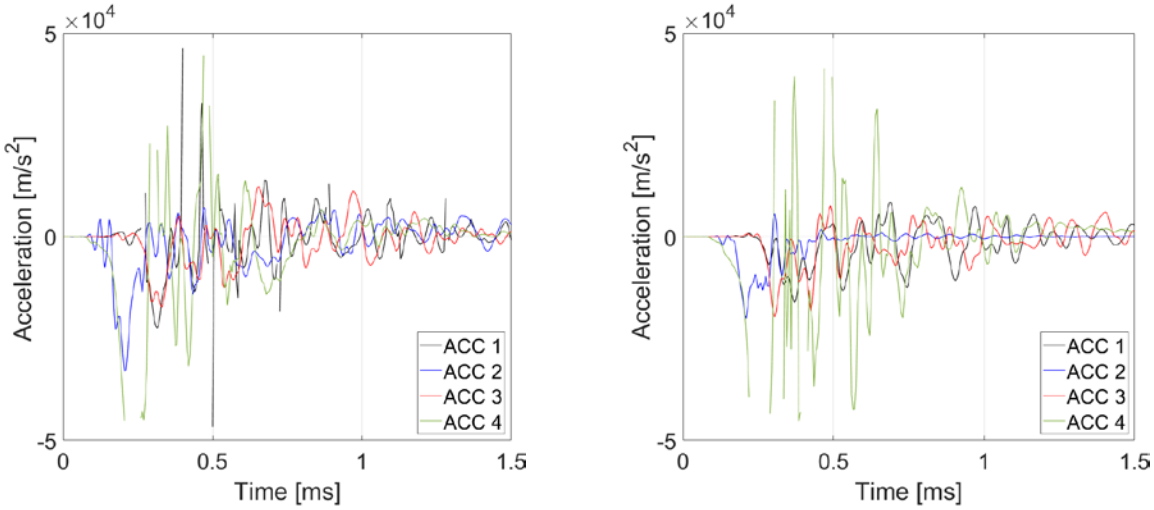

a) S2.1 (without stirrups) tested at 26.2 m/s b) S2.2 (with stirrups) tested at 28.2 m/s

Figure 6. Comparison of acceleration of the beams with and without stirrup reinforcement.

Support forces

The transfer of the impact force towards the supports is one of the mechanisms dissipating the impact energy. The other two are the inertia force of the specimens and the damage evolution within the specimens consuming energy. Therefore, the support forces inversely indicate the damage of the specimens for specimens carried out with comparable impact energies under the assumption that the inertia force was approximately equal in all experiments. The support forces that were measured in the experiments with stirrup-reinforced specimens were indeed higher than in the case of the specimens without stirrup reinforcement. The reason was very likely the lower damage level of the specimens. Additionally, the stiffness of the specimen after the impact is higher, also leading to less localized damage and it might also lead to less acceleration of the separated cone. However, as already mentioned, the maximum acceleration on the punching cone (ACC 4) could not be compared between the different degrees of reinforcement as the senor readings exceeded the measureable limit of the accelerometer. The stirrup-reinforced beams were, however, able to transfer the higher forces towards the supports. The last point also correlates to the generally higher strength of the specimens with stirrup reinforcement.

Another finding was that impactor velocity did not affect the maximum support force. This is the case because the failure mode of the specimens did not change. All experiments were performed above the punching limit (Leicht et al. (2021)). This means that the failure mode was not changed which is why the maximum capacity of the impacted beams remained the same. The capacity of the beams can be correlated to the support force level after the impact.

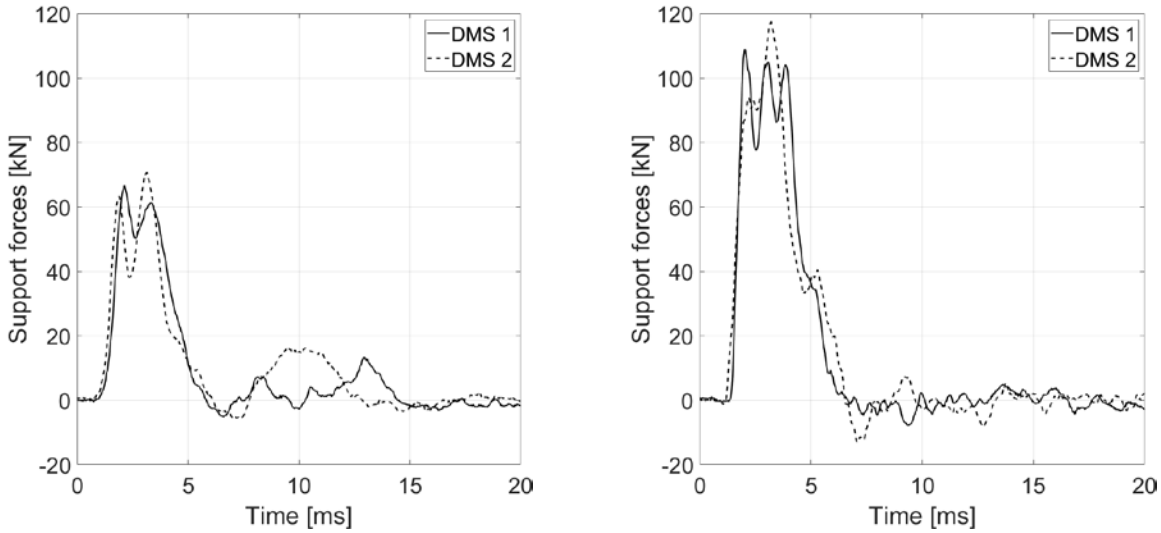

a) S2.1 (without stirrups) tested at 26.2 m/s b) S2.2 (with stirrups) tested at 28.2 m/s

Figure 7. Comparison of support forces of the beams with and without stirrup reinforcement.

Strain distribution

Strain measurements were taken on the reinforcement bars on the bottom reinforcement layer and on some of the stirrups. The position of the strain gauges can be seen in Fig. 1. In almost all experiments, a small minimum or maximum of strains was measured before the strains approached the global maximum. In case the strain measurement was taken in the area of the punching cone cracks, the first strain peak was a local minimum otherwise it was a local maximum. The maximum tensile strains occurred approximately 1 ms to 3 ms after the impact. The time delay was longer for the beams with stirrup reinforcement but in all cases independent of the impactor velocity. There was, therefore, a strong delay between the formation of the first cracks 0.2 ms after the impact and the maximum strains. It is likely that the maximum strains are more dependent on the global bending of the specimen than on the local formation of the punching

cone. The reason is that both deflection on the top side of the specimen and maximum strain were measured between 1.5 ms and 4 ms after the impact. The position of the maximum strains on the longitudinal reinforcement bars was between the centre and the third point of the span. The maximum value and its position along the beam were not affected by the existence of stirrup reinforcement. Above that, the impactor velocity did not affect the maximum strain that was measured. The scattering of the maximum strain measurements between the different experiments was very high. The maximum strains that were measured lied between 1000 µm/m and 4500 µm/m. Again, the equality of the failure mode, the formation of a punching cone, might well be the reason for the independence of the maximum strains from the impactor velocity. A difference between the stirrup-reinforced beams and the beams without stirrup reinforcement was that the maximum strain of the first-named is part of a longer plateau. In the case of the latter, the strains quickly decreased after the maximum strain was observed.

The average of the residual strains was almost equal for the beams with and without stirrup reinforcement. However, the course of the residual strains differed from one another. In the experiments on stirrup-reinforced beams, residual oscillations in the strain gauge measurements were observed. In comparison, the beams without stirrup reinforcement reached an almost constant residual strain (see Fig. 8).

The maximum strain rates that were measured in the approach of the maximum steel strain ranged between 2 1/s and 14 1/s. They were independent of the existence of stirrup reinforcement and loading rate just as the maximum strains.

The strains measured on the stirrup reinforcement were generally smaller than the strains measured on the longitudinal reinforcement bars. The highest strains were measured where the punching cone cracks crossed the stirrup reinforcement but they remained below 2500 µm/m (Leicht et al. (2021)).

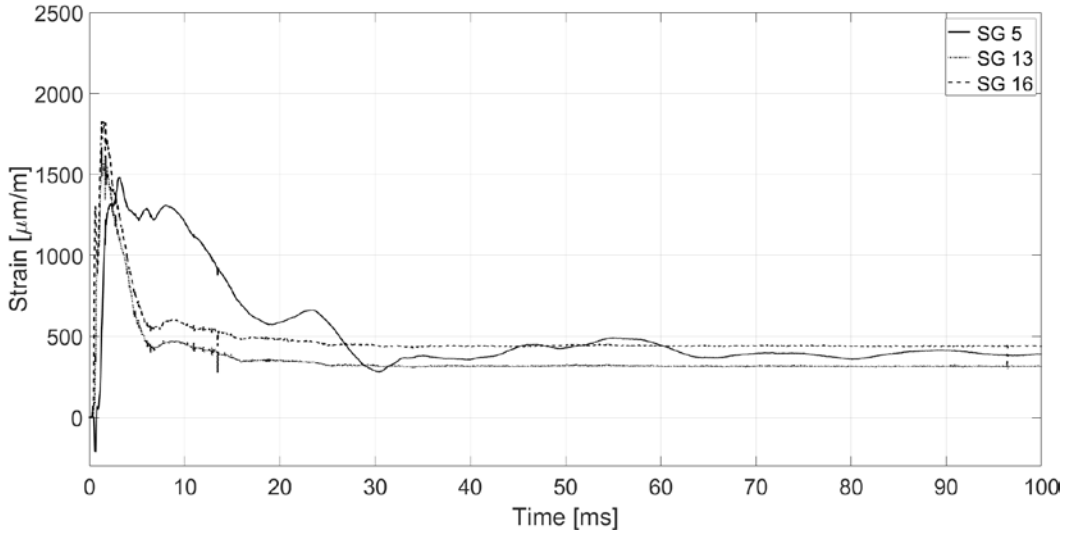

a) S2.1 (without stirrups) tested at 26.2 m/s

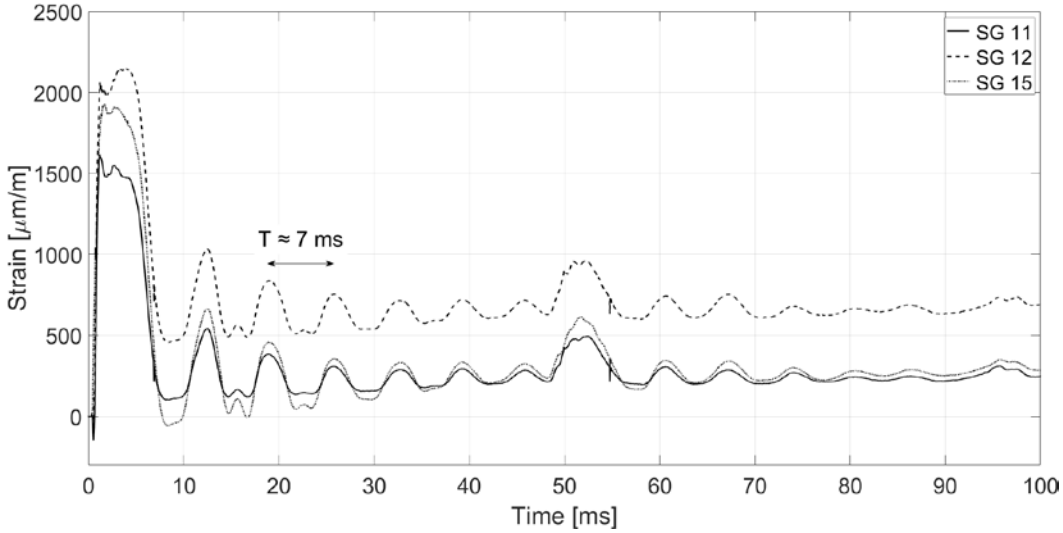

b) S2.2 (with stirrups) tested at 28.2 m/s

Figure 8. Exemplary strain gauge readings with the three highest residual strains. (Leicht et al. (2021))

SUMMARY AND CONCLUSION

In all experiments, the formation of a punching cone was the main failure mode. This failure mode was unaffected by the existence of stirrup reinforcement or the loading velocity in the range of investigation. However, the stirrup reinforcement was capable of holding the specimen together and increasing the stiffness and strength of the specimen. Without stirrup reinforcement, the specimens were separated into a punching cone section and a residual section. With stirrup reinforcement, the body remained whole. This was indicated by the deflection and acceleration measurements showing similar values in the punching cone area and outside of it in the case of stirrup-reinforced beams. Additionally, the support forces of the stirrup-reinforced beams were higher indicating a stiffer response and a higher strength of the specimens. However, looking into the inside of the specimen, the maximum strains were unaffected by the degree of reinforcement. They seemed to be dependent on the global bending of the specimen which was neither affected by the loading velocity nor by the reinforcement. The global bending can be seen in the deformation measurements taken on the top side of the specimen.

All in all, the main difference between beams with and without stirrup reinforcement is the separate movement of the punching cone from the rest of the cross section and the higher strength and stiffness of stirrup-reinforced beam specimens.

The investigation presented in this work allows a better understanding of the behaviour of concrete beams with and without stirrup reinforcement under impact loading. This contributes to evaluation of the impact resistance of concrete structures in NPP.

This work was funded by the German Federal Ministry for Economic Affairs and Climate Action (BMWK) under the grant number 1501566 on the basis of a decision by the German Bundestag and by the Research Training Group GRK 2250 funded by German Research Foundation (Deutsche Forschungsgesellschaft (DFG)).

REFERENCES

Hering, M., Kühn, T., and Curbach, M., Bauteilverhalten unter stoßartiger Beanspruchung durch aufprallende Behälter (Flugzeugtanks) - Phase 1B (Behavior of structural components during impact load conditions caused by tank collisions (aircraft fuel tanks) - Phase 1B) 2017.

Just, M., Curbach, M., Kühn, T. and Hering, M. Bauteilverhalten unter stoßartiger Beanspruchung durch aufprallende Behälter (Flugzeugtanks): Phase 1A (Behavior of structural components during impact load conditions caused by tank collisions (aircraft fuel tanks) - Phase 1A) 2015.

Leicht, L., Beckmann, B. and Curbach, M. (2021). "Influences on the structural response of beams in drop tower experiments," *Civil Engineering Design*, Vol. 3, 5-6, 192-209. https://doi.org/10.1002/cend.202100040

Leicht L., Bracklow F., Hering M., Curbach M. Behaviour of reinforcement in drop tower beam tests. MATEC Web Conf. 2020;323:01007. https://doi.org/10.1051/matecconf/202032301007

Saatci S., Vecchio F.J. (2009). "Effects of shear mechanisms on impact behavior of reinforced concrete beams," *ACI Structural Journal*, 106(1) 78–86. https://doi.org/10.14359/56286.

Soleimani S.M., Roudsari S.S. Analytical study of reinforced concrete beams tested under quasi-static and impact loadings. Journal of Applied Science. 2019;9(14):2838. https://doi.org/10.3390/app9142838

Somraj, A., Fujikake, K. and Li, B. (2013). "Influence of loading rate on shear capacity of reinforced concrete beams," *International Journal of Protective Structures*, Vol. 4, 4, 521-544.

Zhan T., Wang Z., Ning J. Failure behaviors of reinforced concrete beams subjected to high impact loading. Eng Failure Anal. 2015;56: 233–243. https://doi.org/10.1016/j.engfailanal.2015.02.006.